Dr. R. Sutcliffe and D. Lindsay for their advice and technical assistance. This research was supported in part by a grant to L. R. C. B. from the National Science and Engineering Research Council of Canada.

Registry No. 1a, 33888-00-5; **1b**, 82064-85-5; **1c**, 82064-86-6; **2a**, 82064-87-7; **2b**, 82064-88-8; **2c**, 82064-89-9; **3a**, 33887-88-6; **3b**, 82064-90-2; **3c**, 82064-91-3; **6**, 82064-92-4; 3-acetoxy-3-methylbutanoic acid, 44983-17-7; *tert*-butyl 3-acetoxy-3-methylbutyrate, 82064-93-5; 4-hydroxy-4-methyl-1-pentene, 624-97-5; 4-acetoxy-4-methyl-1-pentene, 926-22-7; 3-(benzoyloxy)-3-methylbutanoic acid, 82064-94-6; 3-(cyclopropylcarboxy)-3-methylbutanoic acid, 82064-95-7; cyclopropanecarbonyl chloride, 4023-34-1; 4-(cyclopropylcarboxy)-4-methyl-1-pentene, 82064-96-8; 1-bromo-2-(cyclopropylcarboxy)-2-methylpropane, 82064-97-9; 2-phenyl-4,4-dimethyl-1,3-dioxolan, 52129-02-9; 2-cyclopropyl-4,4-dimethyl-1,3-dioxolan, 82064-98-0.

Supplementary Material Available: Tables of kinetic data (5 pages). Ordering information is given on any current masthead page.

Characterization of the 1:1 Charge-Transfer Reaction between Decamethylferrocene and 2,3-Dichloro-5,6-dicyanoquinone (DDQ): Structure of the $DDQH^-$ Anion[1]

Elizabeth Gebert,[2] A. H. Reis, Jr.,*[3] Joel S. Miller,*[4a] Heiko Rommelmann,[4b] and Arthur J. Epstein[4b]

Contribution from the Chemistry Division, Argonne National Laboratory, Argonne, Illinois 60439, Department of Chemistry, Brandeis University, Waltham, Massachusetts 02254, the Occidental Research Corporation, Irvine, California 92713, and the Xerox Webster Research Center, Rochester, New York 14644. *Received May 28, 1981*

Abstract: The 1:1 charge-transfer reaction of decamethylferrocene (DMeFc) and 2,3-dichloro-5,6-dicyanoquinone (DDQ) results in a heterosoric stacked complex of $[DMeFc^{+}\cdot][DDQH^-]$ composition where the $DDQH^-$ anion has a structure intermediate between the quinoid and benzenoid states. The crystal structure of the 1:1 complex $[DMeFc^{+}\cdot][DDQH^-]$ has been determined by single-crystal X-ray diffraction. The material crystallizes in the orthorhombic space group, *Pbna*, with unit cell parameters $a = 17.027$ (3) Å, $b = 14.497$ (4) Å, $c = 10.616$ (1) Å, $V = 2620.4$ (14) Å^3, $Z = 4$, $\rho_c = 1.40$ g cm^{-3}. The data were collected on a four-circle Syntex $P2_1$ diffractometer, and the structure was solved by direct methods and refined with Fourier and full-matrix least-squares techniques. The final R_F was 0.054 for 2409 independent reflections where $F^2_{obsd} > \sigma F^2_{calcd}$. The crystal structure consists of heterosoric stacks of alternating $DMeFc^{+}\cdot$ and $DDQH^-$ ions along the c axis. Each ion has C_2 symmetry, the $DDQH^-$ ion being disordered. The planar $DDQH^-$ anion and C_5Me_5 rings of the $DMeFc^{+}\cdot$ ion are separated by 3.564 Å. The angle between the C_5 and $DDQH^-$ plane is 3.33°. The structure of the $DDQH^-$ ion is intermediate between the quinoid and benzenoid states with C=C bond distances of 1.368 (5) and 1.384 (4) Å and C–C bond distances of 1.454 (3) and 1.445 (3) Å. The C=O, C—Cl, and C≡N distances are 1.237 (3), 1.732 (2), and 1.101 (3) Å, respectively. The $DMeFc^{+}\cdot$ is ordered, and the C_5Me_5 rings are staggered by 26° with the methyl groups directed away from the Fe atom and out of the C_5Me_5 plane by 0.30–0.74 Å. The average Fe–C, C–C, and C–Me bond distances are 2.096 (2), 1.422 (3), and 1.505 (3) Å, respectively. The spin susceptibility at room temperature is 5.00×10^{-3} emu/mol or 3.5 μ_B for fully oriented samples ($g_\parallel$ of $DMcFe^{+}\cdot$ parallel to the magnetic field). This is consistent with a $S = {}^1/_2$ $DMeFc^{+}\cdot$, which possesses $g_\perp = 1.92$ and $g_\parallel = 4.002$. The magnetic susceptibility fits the Brillouin function for all temperatures studied (≥1.80 K) and for magnetic fields up to 8 T. There is no evidence for exchange coupling among the $DMeFc^{+}\cdot$ spins, in contrast to the behavior observed for $(DMeFc^{+}\cdot)(TCNQ^{-}\cdot)$. Comparison of the magnetic properties of these two compounds demonstrates the important role of the presence of a spin on the acceptor molecule in mediating the exchange interaction between $DMeFc^{+}\cdot$ units.

We have recently characterized several major products formed from the charge-transfer reaction of decamethylferrocene (DMeFc) and 7,7,8,8-tetracyano-*p*-quinodimethane (TCNQ) that have interesting chemical and physical properties.[5-8] In these charge-transfer reactions involving TCNQ, the resulting electron-rich $TCNQ^{-}\cdot$ radical anion shows structural differences when compared to the unperturbed neutral TCNQ molecule. These differences are predominantly manifested in the lengthening of the exocyclic carbon–carbon double bonds with charge transfer of electron density from the donor to acceptor.[8b] The exact amount of charge transferred, however, is difficult to ascertain from any bond length correlation.[8b,c]

The analogous charge-transfer reaction of ferrocene and 2,3-dichloro-5,6-dicyanoquinone (DDQ) was initially described as forming a phenoxy radical ion.[9] This reaction was of interest because of the comparable strength of DDQ (electron affinity, $E_A \sim 3$ eV)[11] as an organic electron acceptor when compared to TCNQ[9,10] ($E_A = 2.8$ eV).[11] No direct structural information was available as to the nature of the phenoxy radical ion, which was postulated and later reformulated to be the hydroquinonide

(1) Research performed under the auspices of the Division of Basic Energy Sciences, U.S. Department of Energy.
(2) Argonne National Laboratory.
(3) Brandeis University, Waltham, MA 02254.
(4) (a) Occidental Research Corp. (b) Xerox Corp.
(5) Candela, G. A.; Swartzendruber, L. J.; Miller, J. S.; Rice, M. J. *J. Am. Chem. Soc.* **1979**, *101*, 2755.
(6) Reis, A. H., Jr.; Preston, L. D.; Williams, J. M.; Peterson, S. W.; Miller, J. S. *J. Am. Chem. Soc.* **1979**, *101*, 2756.
(7) Miller, J. S.; Reis, A. H., Jr.; Candela, G. *Lect. Notes Phys.* **1979**, *96*, 313.
(8) (a) Miller, J. S.; Reis, A. H., Jr.; Gebert, E.; Ritsko, J. J.; Salaneck, W. R.; Kovnat, L.; Cape, T. W.; Van Duyne, R. P. *J. Am. Chem. Soc.* **1979**, *101*, 711. (b) Wilson, S. R.; Corvan, P. J.; Seiders, R. P.; Hodgson, D. J.; Brookhart, M.; Hatfield, W. E.; Miller, J. S.; Reis, A. H., Jr.; Rogan, P. K.; Gebert, E.; Epstein A. J. In "Molecular Metals"; Hatfield, W. E., Ed.; Plenum Press: **1979**. (c) Reis, A. H., Jr.; Rogan, P. K.; Gebert, E.; Wilson, S. R.; Corvan, P. J.; Seiders, R. P.; Hodgsen, D. J.; Brookhart, M.; Hatfield, W. E.; Epstein, A. J.; Cope, T. W.; Van Duyne, R. P.; Chaikin, P. M.; Miller, J. S., manuscript in preparation. (d) Willi, C.; Reis, A. H., Jr.; Gerbert, E.; Miller, J. S. *Inorg. Chem.* **1981**, *20*, 313.
(9) Brandon, R. L.; Osiecki, J. H.; Ottenberg, A. *J. Org. Chem.* **1966**, *31*, 1214.
(10) Herbstein, F. H. In "Perspective in Structural Chemistry", Dunitz, J. D., Ibers, J. A. Eds.; Wiley: New York, 1971, p 166.
(11) Kampars, V.; Neiland, O. *Russ. Chem. Rev.* **1977**, *46*, 503-513.

0002-7863/82/1504-4403$01.25/0

Table I. Experimental Details of [DMeFc^{+}·][DDQH^{-}]

cell constants at 20 °C, a 17.027 (3), b 14.497 (4), c 10.616 (2) A
cell volume: 2620.4 (14) A^3
mol wt, 554.2
calcd density, 1.40 gm cm^{-3}
obsd density, 1.39 gm cm^{-3}
Z 4
space group, $Pbna$ (D_{2h}^{14}, No. 60)
radiation, Mo K$\bar{\alpha}$, λ = 0.71069 A
max 2θ, 55.0 ° (h,k,l)
scan type θ–2θ coupled
scan width, $(1.9 + (\alpha_2 - \alpha_1))^\circ$
scan speed, variable 1.96–29.30 deg/min
crystal
V, 5.98 × 10^{-5} cm^3 (0.07 × 0.03 × 0.03 cm)
absorption coefficient, 8.219 cm^{-1}
max. transmission factor, 0.80
min. transmission factor, 0.75
no. of reflctns collected 3684
no. of independent reflctns 3042
R_F 0.054 for 2409 reflctns with $F^2_o > \sigma F^2_c$
GOF 1.414

DDQH^{-} diamagnetic anion.[12] We present here the structural and magnetic characterization of the reaction of decamethylferrocene and DDQ and discuss the nature of the hydroquinonide DDQH^{-} anion that is formed.

Experimental Section

Preparation of [Fe(C$_5$(CH$_3$)$_5$)]$^{+}$·[DDQH]$^{-}$. A warm filtered acetonitrile solution containing 111.3 mg of DMeFc (0.341 mmol) was added to a hot filtered acetonitrile solution containing 77.9 mg of freshly recrystallized DDQ (from chloroform under Ar, Aldrich, 0.343 mmol). The pair of amber solutions turned deep purple on mixing, and the warm solution was permitted to slowly cool in a preheated Dewar to ambient temperature. After 48 h 60.0 mg (32%) of purple needle crystals was harvested via vacuum filtration. All operations were carried out in a Vacuum Atmospheres HE553 Dri-Lab. The acetonitrile utilized was dried via distillation over phosphorus pentoxide[13] in an argon atmosphere. Reaction of 1:2 DMeFc:DDQ lead to the isolation of the 1:1 identical product (50% yield).

Magnetic Properties. The magnetic susceptibility, χ, was measured by utilizing the Faraday technique. Measured samples (typically ~50 mg) were contained in a bucket (~20 mg) formed from 0.99999 aluminum foil or a calibrated gold-coated gelatin capsule and suspended by a 50-μm diameter tungsten wire from a Perkin-Elmer AR-2 electrobalance. Magnetic fields, H, up to 8 T (uniform to 1 part in 10^5 over 1 cm) are supplied by an American Magnetics, Inc. (AMI), superconducting magnet. A second superconducting magnet provides field gradients up to ±0.08 T/cm. (The gradient is uniform to 1 part in 10^3 over 1 cm.) Temperature (T) control was provided by a Janis Research Corp. "Supervaritemp" Dewar. The calibration of the instrument was verified by measurement of an aluminum standard obtained from the National Bureau of Standards. The data were obtained by monitoring the force on the sample while the sign of dH/dz was alternated. This technique permits virtually continuous data collection while magnetic field or temperature is varied. The sample holder was calibrated separately as a function of temperature, and the value of its susceptibility is subtracted from the measured value at each point.

X-ray Data Collection. A single crystal of [DMeFc^{+}·][DDQH^{-}] was sealed in a glass capillary and mounted on a Syntex P2$_1$ automatic diffractometer under control of a NOVA computer. Cell orientation, unit cell parameters, and crystal quality were determined as described previously.[14] The crystal system is orthorhombic with unit cell parameters a = 17.027 (3) Å, b = 14.497 (4) Å, c = 10.616 (2) Å, V = 2620.4 (14) Å^3, and Z = 4.

Three reflections were chosen as standard reflections to be monitored every 80 reflections as a guide to the stability of the system and crystal. After 80 h of data collection, the intensity of the check reflections decreased significantly (~10%). The crystal was realigned and the data collection was resumed. The drop in intensity was found to be real. The total data collection required approximately 90 h. Intensity data were collected in one octant to a 2θ maximum of 55°. Systematic absences were consistent with space group $Pbna$, a nonstandard setting of space group $Pbcn$ (No. 60, D_{2h}^{14}). Experimental information is summarized in Table I.

Solution and Refinement of Structure. Absorption and Lorentz and polarization corrections were applied to the data by the program DATALIB.[15] Due to the change of intensity in the check reflections, the data were normalized in DATALIB to the interpolated value of the sum of the net counts of the standard reflections and the equivalent reflections averaged in the program DATASORT.[15] Statistical tests in the direct methods program, MULTAN74, indicated the space group to be centrosymmetric.[16] The structure of the decamethylferrocenium radical cation was clearly shown by MULTAN74. The subsequent structure factor calculation and three-dimensional Fourier analysis clearly located the non-hydrogen atoms of the DDQH^{-} moiety. A full-matrix least-squares refinement of all non-hydrogen atoms with isotropic thermal parameters yielded an R_F value of 0.168 for all reflections. Further refinement of anisotropic thermal parameters on all non-hydrogen atoms reduced the R_F value to 0.099. A difference Fourier analysis enabled 12 of the 15 methyl hydrogen atoms to be located. Adding the 12 hydrogens to the least-squares refinement reduced the R_F to 0.083, and a subsequent difference Fourier map revealed the 3 remaining methyl hydrogens. A final difference Fourier revealed electron density (0.32 e/Å^3) at a distance of 1.04 Å from the quinone oxygen. This electron density was subsequently labeled H(6). The C(7)–O(1)–H(6) angle is 140.2°. The electron density of 0.32 e/Å^3 and the space group symmetry demand that H(6) is disordered about the C_2 axis of the quinone. The closest approach of H(6) to any other atom is 2.14 Å to C(7) and 2.30 Å to the hydrogen of the nearest methyl group. A full-matrix least-squares refinement of all 33 non-hydrogen atoms with anisotropic thermal parameters and the nonquinoid hydrogen atoms with isotropic thermal parameters were refined to a final R_F of 0.073 for all 3042 reflections, and R_F = 0.054 for 2409 reflections where $F^2_o > \sigma F^2_c$. The goodness of fit, GOF, was 1.41 for all reflections. There was no evidence of extinction. The highest residual electron density on the final difference Fourier map was 0.53 e/A^3. The atomic positions and thermal parameters are given in Table II. The observed vs. calculated structure factors are given as supplementary material. The quantity minimized during refinement was $w|F^2_o - F^2_c|$, where F_o and F_c are the observed and calculated structure amplitudes, respectively. Weights were assigned as $w = 1/(\sigma F^2_o)^2$, $\sigma(I) = [SC + \tau^2(B_1 + B_2) + P^2I^2]^{1/2}$ where SC is the scan count, τ is the scan to background time ratio, B_1 and B_2 are the background counts on each side of a peak, I is the net intensity, and P is a systematic error factor set at 0.03, a value found to be appropriate in this laboratory. The agreement indices are

$$R_F = ||F_o| - |F_c||/\Sigma|F_o| \quad (1)$$

$$\text{GOF} = [\Sigma w|F^2_o - F^2_c|^2/(N_o - N_r)]^{1/2} \quad (2)$$

where N_o is the number of independent reflections and N_r is the number of parameters varied. The programs not previously mentioned that were used are S5XFLS[17] and S5FOUR[17] for least-squares refinement and Fourier calculations. The bond distances and angles were calculated with S5FFE.[17] The LSPLANE program[18] was used to calculate the least-square planes and atomic distances from the planes. ORTEP[19] was used to construct molecular drawings. Scattering factors were taken from a compilation of Cromer and Weber[20] and were modified for the real and imaginary components of anomalous dispersion.

Results

Structure Description. The crystal structure consists of stacks of equally spaced DMeFc^{+}· and DDQH^{-} ions separated by 3.564 Å along the c axis of the crystal. Due to disorder both ions have apparent C_2 point symmetry and lie on the 2-fold axis of rotation parallel to a. This forces only one-half of the atoms of each ion to be unique. The stacking is shown in Figure 1, and stereoviews of the stacking within the unit cells are shown in Figures 2 and

(12) (a) Morrison, Jr., W. H.; Krogsrud, S.; Hendrickson, D. N., *Inorg. Chem.* **1973**, *12*, 1998. (b) Morrison, W. H., Jr.; Hendrickson, D. N. *Inorg. Chem.* **1975**, *14*, 2331.

(13) Melby, L. R.; Harder, R. J.; Hertler, W. R.; Mahler, W.; Benson, R. E.; Mochel, W. E. *J. Am. Chem. Soc.* **1964**, *84*, 3374.

(14) Reis, A. H., Jr.; Willi, C.; Siegel, S.; Tani, B. *Inorg. Chem.* **1979**, *18*, 1859.

(15) DATALIB and DATASORT were written by H. A. Levy and locally adopted for the IBM 370/195.

(16) MULTAN74 was written by P. Main, M. M. Wolfson, and G. Germain and locally adopted for the IBM 370/195.

(17) S5FOUR, S5XFLS, and S5FFE are Sigma 5 versions of the programs FOURIER by R. J. Dellaca and W. T. Robinson, ORXFLS by W. R. Busing and H. A. Levy, and ORFFE3 by W. R. Busing and H. A. Levy, respectively.

(18) LS PLANES was written by M. E. Pippy.

(19) ORTEP was written by C. Johnson.

(20) "International Tables for X-ray Crystallography"; Kynoch Press: Birmingham, England, 1974; Vol. IV: (a) p 71; (b) p 102; (c) p 148.

Table II. Positional Atomic Coordinates and Isotropic and Anisotropic Thermal Parameters[a,b] for [DMeFc⁺·][DDQH⁻]

atom	x	y	z	U_{11}	U_{22}	U_{33}	U_{12}	U_{13}	U_{23}
Fe	0.14086 (2)	0.75	0.5	0.030 (0)	0.031 (0)	0.027 (9)	0.0	0.0	0.001 (0)
C1	0.0719 (1)	0.7441 (2)	0.3365 (2)	0.033 (1)	0.048 (1)	0.029 (1)	−0.002 (1)	−0.003 (1)	0.001 (1)
C2	0.1044 (1)	0.8339 (1)	0.3503 (2)	0.053 (1)	0.037 (1)	0.030 (1)	0.008 (1)	−0.002 (1)	0.003 (1)
C3	0.1875 (1)	0.8252 (2)	0.3490 (2)	0.049 (1)	0.051 (1)	0.029 (1)	−0.015 (1)	0.003 (1)	0.003 (1)
C4	0.2063 (1)	0.7301 (1)	0.3353 (2)	0.035 (1)	0.055 (2)	0.032 (1)	0.005 (1)	0.005 (1)	0.002 (1)
C5	0.1345 (1)	0.6800 (1)	0.3272 (2)	0.050 (1)	0.035 (1)	0.028 (1)	0.000 (1)	0.002 (1)	0.000 (1)
Me1	−0.0140 (2)	0.7197 (3)	0.3297 (3)	0.040 (1)	0.099 (3)	0.054 (2)	−0.010 (1)	−0.008 (1)	−0.004 (2)
Me2	0.0581 (2)	0.9229 (2)	0.3569 (3)	0.096 (3)	0.049 (2)	0.056 (2)	0.029 (2)	−0.004 (2)	0.005 (1)
Me3	0.2444 (2)	0.9045 (3)	0.3543 (3)	0.097 (3)	0.074 (2)	0.058 (2)	−0.048 (2)	0.011 (2)	0.002 (2)
Me3	0.2877 (2)	0.6905 (3)	0.3261 (3)	0.047 (2)	0.110 (3)	0.056 (2)	0.023 (2)	0.011 (1)	−0.003 (2)
Me3	0.1268 (3)	0.5783 (2)	0.3066 (3)	0.116 (3)	0.037 (1)	0.050 (2)	−0.003 (2)	0.003 (2)	−0.007 (1)
C6	0.0649 (1)	0.7034 (2)	−0.0103 (2)	0.047 (1)	0.087 (2)	0.039 (1)	−0.008 (1)	−0.002 (1)	−0.001 (2)
C7	0.1366 (1)	0.6497 (2)	−0.0230 (2)	0.058 (1)	0.061 (2)	0.038 (1)	−0.012 (1)	−0.001 (1)	0.002 (1)
C8	0.2079 (1)	0.7030 (1)	−0.0114 (2)	0.049 (1)	0.045 (1)	0.036 (1)	−0.001 (1)	0.000 (1)	0.003 (1)
C9	0.2811 (2)	0.6541 (2)	−0.0219 (2)	0.060 (1)	0.039 (1)	0.050 (2)	−0.005 (1)	−0.002 (1)	−0.004 (1)
Cl	−0.0214 (0)	0.6406 (1)	−0.0203 (1)	0.055 (0)	0.131 (1)	0.081 (1)	−0.027 (0)	0.004 (0)	−0.018 (1)
O	0.1371 (1)	0.5649 (1)	−0.0428 (2)	0.074 (1)	0.060 (1)	0.076 (1)	−0.017 (1)	−0.005 (1)	−0.003 (1)
N	0.3382 (1)	0.6189 (2)	−0.0290 (2)	0.067 (1)	0.054 (1)	0.088 (2)	0.001 (1)	−0.003 (1)	−0.012 (1)
H11	−0.043 (2)	0.774 (2)	0.369 (3)	8.7 (10)					
H12	−0.027 (2)	0.672 (2)	0.380 (3)	8.6 (10)					
H13	−0.028 (2)	0.710 (2)	0.247 (3)	7.0 (8)					
H21	0.057 (2)	0.950 (2)	0.266 (3)	8.9 (9)					
H22	0.093 (2)	0.972 (2)	0.403 (3)	9.2 (10)					
H23	0.006 (2)	0.914 (2)	0.393 (3)	8.9 (10)					
H31	0.232 (2)	0.945 (2)	0.415 (4)	9.9 (12)					
H32	0.299 (2)	0.876 (3)	0.378 (4)	10.1 (12)					
H33	0.253 (2)	0.932 (2)	0.271 (3)	9.3 (10)					
H41	0.302 (2)	0.686 (2)	0.238 (3)	7.8 (8)					
H42	0.324 (2)	0.719 (2)	0.383 (4)	8.2 (9)					
H43	0.287 (2)	0.628 (2)	0.354 (3)	7.2 (9)					
H51	0.128 (2)	0.568 (2)	0.218 (4)	8.6 (9)					
H52	0.087 (2)	0.554 (2)	0.357 (4)	9.9 (12)					
H53	0.159 (2)	0.552 (2)	0.364 (4)	10.4 (12)					
H6	0.166	0.516	−0.097	5.0					

[a] The form of the anisotropic temperature factor is $\exp[-2\pi^2(U_{11}h^2a^{*2} + \ldots + 2U_{23}klb^*c^*)]$. [b] Estimated standard deviations are given in parentheses.

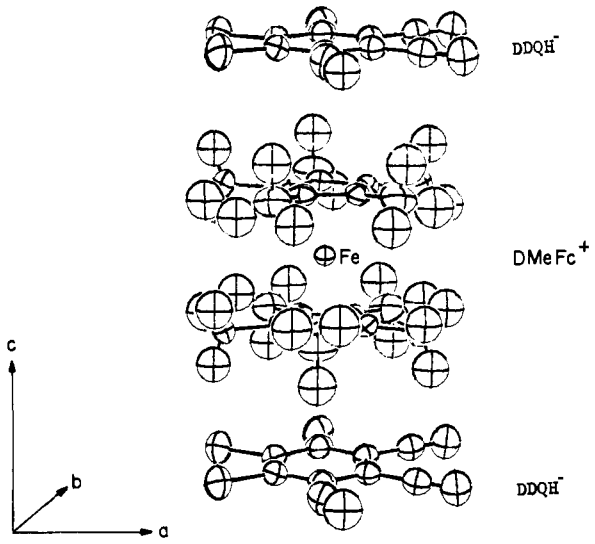

Figure 1. Heterosoric stacking of DDQH⁻ and DMeFc⁺· along the *c* axis of the crystal. Only one configuration of disordered DDQH⁻ ion is shown. The hydrogen atom has been drawn with an approximated isotropic thermal ellipsoid of $B = 5$ Å^2.

Table III. Interatomic Distances in [DMeFc⁺·][DDQH⁻] with Estimated Standard Deviations Given in Parentheses

atoms	distance, A	atoms	distance, A
A. Distances within DMeFc⁺·			
Fe-C(1)	2.097 (2)	Me(1)-H(11)	1.02 (3)
Fe-C(2)	2.095 (2)	Me(1)-H(12)	0.91 (3)
Fe-C(3)	2.095 (2)	Me(1)-H(13)	0.92 (3)
Fe-C(4)	2.093 (2)	Me(2)-H(21)	1.04 (4)
Fe-C(5)	2.099 (2)	Me(2)-H(22)	1.05 (4)
C(1)-C(2)	1.422 (3)	Me(2)-H(23)	0.98 (3)
C(2)-C(3)	1.421 (3)	Me(3)-H(31)	0.89 (4)
C(3)-C(4)	1.424 (3)	Me(3)-H(32)	1.05 (3)
C(4)-C(5)	1.424 (3)	Me(3)-H(33)	0.98 (4)
C(5)-C(1)	1.418 (3)	Me(4)-H(41)	0.97 (3)
C(1)-Me(1)	1.507 (3)	Me(4)-H(42)	0.96 (4)
C(2)-Me(2)	1.513 (3)	Me(4)-H(43)	0.95 (3)
C(3)-Me(3)	1.505 (3)	Me(5)-H(51)	0.96 (4)
C(4)-Me(4)	1.503 (3)	Me(5)-H(52)	0.93 (4)
C(5)-Me(5)	1.497 (3)	Me(5)-H(43)	0.90 (4)
B. Distances within DDQH⁻			
C(6)-C(6')	1.368 (5)	C(8)-C(9)	1.438 (3)
C(6)-C(7)	1.454 (3)	C(9)-N(1)	1.101 (3)
C(7)-C(8)	1.445 (3)	C(6)-Cl(1)	1.732 (3)
C(8)-C(8')	1.384 (4)	C(7)-O(1)	1.247 (3)
		O(1)-H(6)	1.04

3. The DDQH⁻ ion, Figure 4, exhibits an approximate quinoidal geometry where the C_2 axis of symmetry lies along the midpoints of the C(8)-C(8′) and C(6)-C(6′) "double" bonds of the six-membered rings. These double bond distances are 1.384 (4) and 1.368 (5) Å, respectively. The four "single" bonds have two unique distances of C(6)-C(7) = 1.454 (3) Å and C(7)-C(8) = 1.445 (3) Å. The quinoidal C(7)-O, C(6)-Cl, and C(8)-C(9) bond distances are 1.247 (3), 1.732 (2), and 1.438 (3) Å, respectively. The C(9)-N triple bond distance is 1.101 (3) Å while the C-(8)-C(9)-N bond angle is 178.0 (3)°. The six-carbon quinone ring is planar to within ±0.006 (2) Å. The Cl atoms are ±0.052 (1) Å and the O atoms are ±0.002 Å from the least-squares plane while the C(9) and N atoms are located ±0.002 (2) Å and ±0.012 (3) Å from the planes, respectively. The disordered hydroquinonide hydrogen is 1.04 Å from the oxygen, O(1), and the C(7)-O(1)-H(6) angle is ~140.2°.

The decamethylferrocenium ion lies on the C_2 axis where the Fe atom is located at the special crystallographic position (0.14086, $^3/_4$, $^1/_2$) forcing only one of the five-membered ring moieties to be unique. The average Fe-C, C-C, and C-Me bond distances

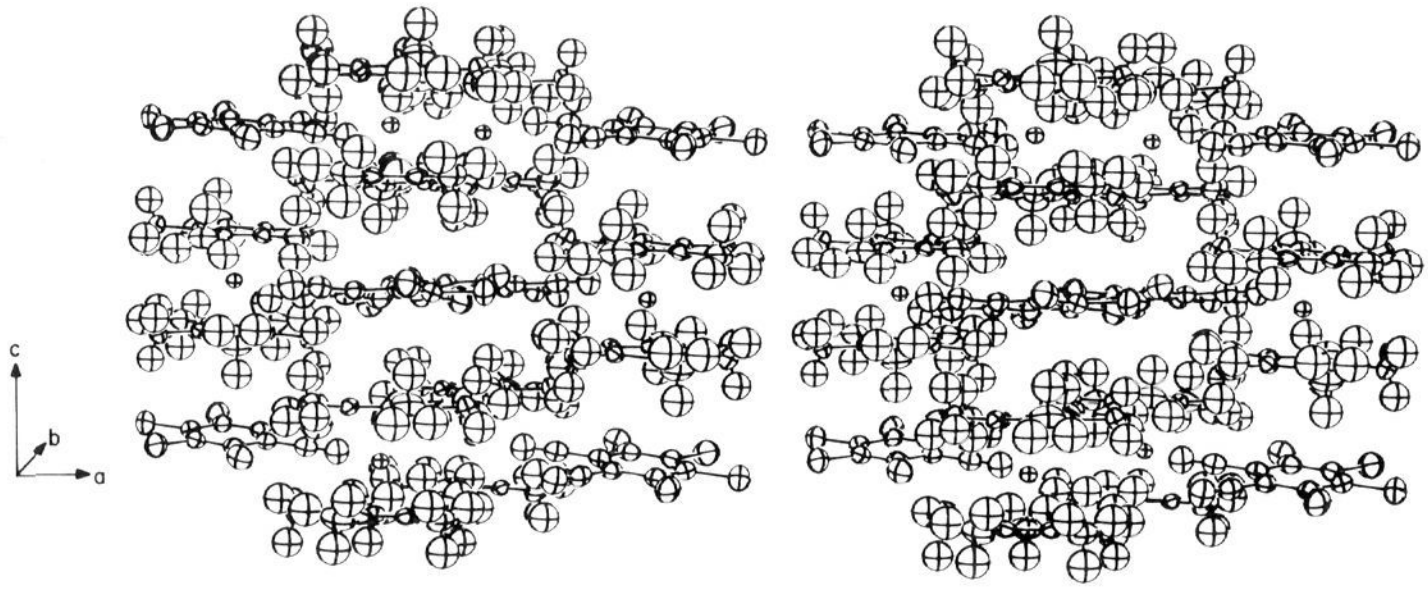

Figure 2. Stereoview of the unit cell which illustrates the stacking of the ions along the *c* axis. The dark circles are the iron atoms. The disordered $DDQH^-$ hydrogen atom has been omitted.

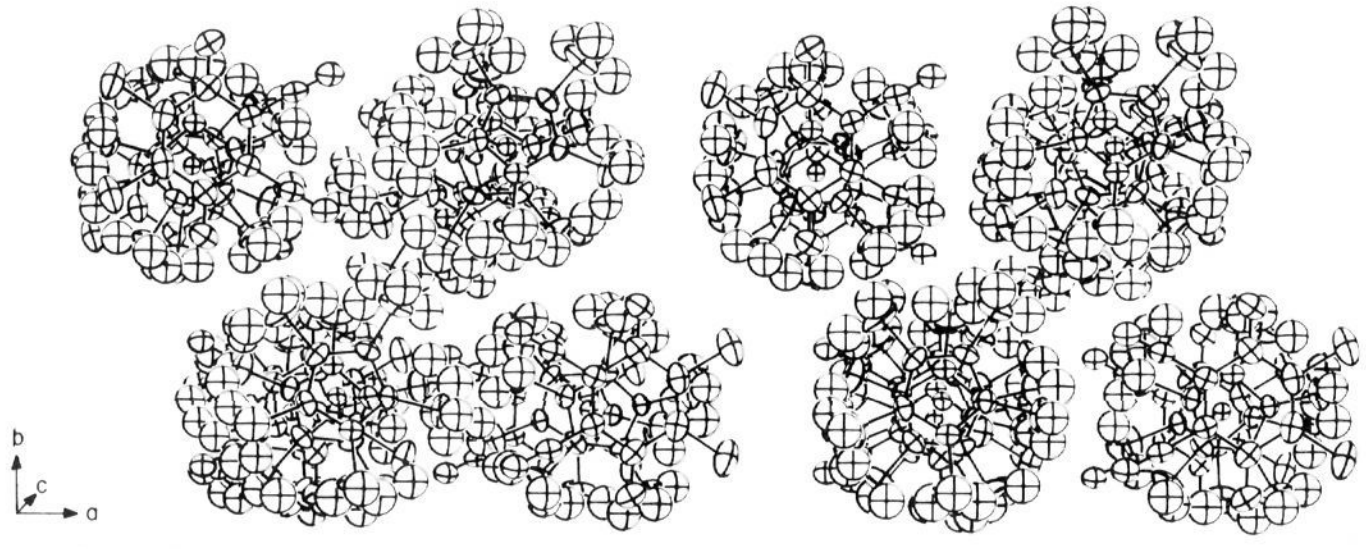

Figure 3. Stereoview of the unit cell illustrating the stacking along the *b* axis. The disordered $DDQH^-$ hydrogen atom has been omitted.

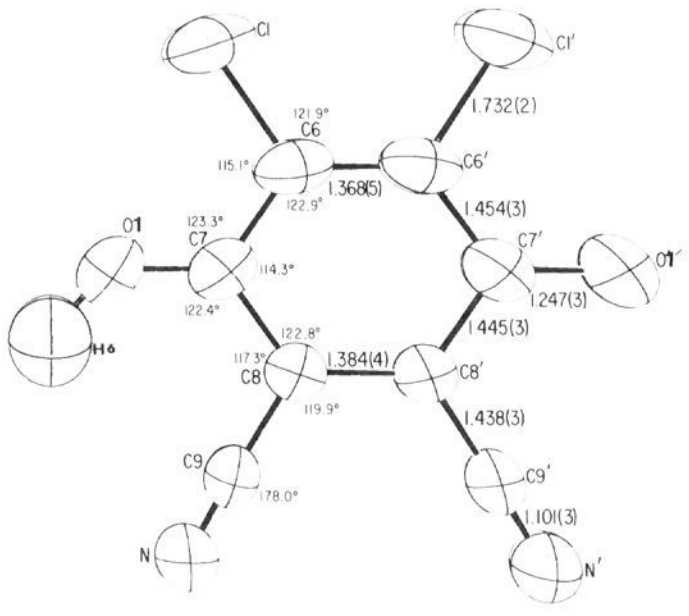

Figure 4. $DDQH^-$ ion showing the bond lengths and angles. Only one configuration of the disordered $DDQH^-$ ion is shown. The hydrogen atom has been drawn with an approximated isotropic thermal ellipsoid of $B = 5.0$ Å^2.

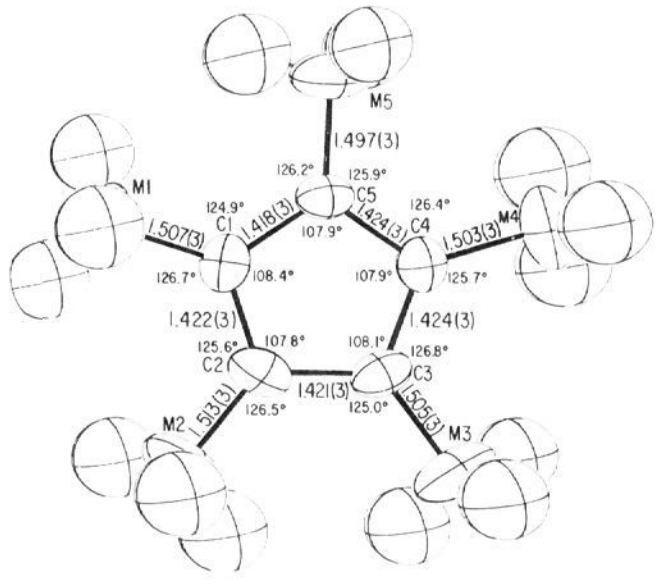

Figure 5. $DMeFc^{+\cdot}$ ion showing the non-hydrogen bond lengths and bond angles. Notice the similarity in magnitude of all lengths and angles. The hydrogen atoms have been drawn with an assigned value of $B = 5.0$ Å^2.

(Figure 5 and Table III) are 2.096 (2) 1.422 (3), and 1.505 (3) Å, respectively. The C_5 ring bond angles (Table IV) correspond to a regular planar pentagon, i.e., 108.0 ± 0.4°. The carbon atoms of the C_5 ring are within ±0.003 (2) of the least-squares plane with the methyl carbon atoms lying between 0.030 (3) and 0.074 (4) Å above the C_5 plane and away from the Fe atom, which is 1.712 (2) Å from the C_5 plane. The C_5Me_5 ring shows a 26° twist angle compared to the staggered configuration of 36°. Two of the three hydrogen atoms of each methyl group lie below the least-squares plane and toward the Fe atom (Figures 1–3, 5). The C–H bond distances are in the range of those found in the literature[14] of refined X-ray structures. The C_5 ring of the C_5Me_5 moiety and the quinone six-membered ring are not parallel but show a tilt angle of 3.33° with respect to each ring.

Magnetic Studies. The magnetic susceptibility, χ, was measured by utilizing the Faraday technique. This technique measures the total magnetic susceptibility including the diamagnetic cores of the DMeFc° and DDQ° molecules. The diamagnetic core corrections for DMeFc° and DDQ° were obtained experimentally (Figures 6 and 7). Analysis of the Honda plots for the neutral DMeFc°, Figure 8, and DDQ°, Figure 9, demonstrated less than 3 ppm ferromagnetic impurity in each case. The intrinsic temperature-independent diamagnetism, χ_{core}, for DMeFc° and DDQ° was obtained by fitting the temperature-dependent susceptibility data to

$$\chi_{meas} = \chi_{core} + C/T \qquad (3)$$

The second term on the right hand-side accounts for the small

Table IV. Interatomic Bond Angles in [DMeFc⁺·][DDQH⁻] with Estimated Standard Deviations Given in Parentheses

atoms	angles, deg	atoms	angles, deg
A. Angles within the DMeFc⁺·			
C(5)-C(1)-C(2)	108.4 (2)	C(1)-C(2)-Me(2)	125.6 (2)
C(3)-C(2)-C(1)	107.8 (2)	C(2)-C(3)-Me(3)	125.0 (3)
C(2)-C(3)-C(4)	108.1 (2)	C(4)-C(3)-Me(3)	126.8 (3)
C(3)-C(4)-C(5)	107.9 (2)	C(3)-C(4)-Me(4)	125.7 (2)
C(1)-C(5)-C(4)	107.9 (2)	C(5)-C(4)-Me(4)	126.4 (3)
C(5)-C(1)-Me(1)	124.9 (2)	C(1)-C(5)-Me(5)	126.2 (3)
C(2)-C(1)-Me(1)	126.7 (2)	C(4)-C(5)-Me(5)	125.9 (3)
C(3)-C(2)-Me(2)	126.5 (2)		
B. Angles within the DDQH⁻			
C(6')-C(6)-C(7)	122.9 (1)	C(8)-C(7)-O(1)	122.4 (2)
C(8)-C(7)-C(6)	114.3 (2)	C(6)-C(7)-O(1)	123.3 (2)
C(8')-C(8)-C(7)	122.8 (1)	C(8')-C(8)-C(9)	119.9 (1)
C(6')-C(6)-Cl	121.9 (1)	C(7)-C(8)-C(9)	117.3 (2)
C(7)-C(6)-Cl	115.1 (2)	C(8)-C(9)-N	178.0 (3)
		C(7)-O(1)-H(6)	140.2

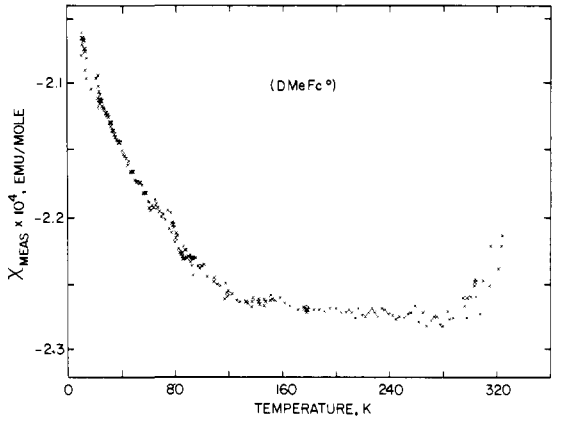

Figure 6. Molar susceptibility vs. temperature for DMeFc.

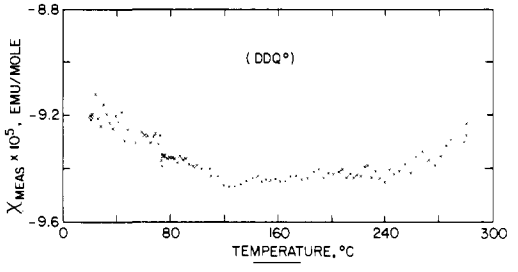

Figure 7. Molar susceptibility vs. temperature for DDQ°.

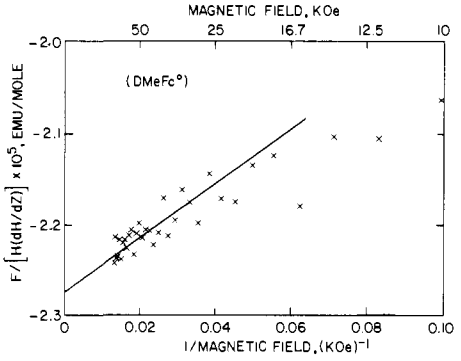

Figure 8. Honda plot for DMeFc° (F = force, H = magnetic field, dH/dz = magnetic field gradient).

Curie-like upturn characteristic of extrinsic Curie impurities commonly found in donor and acceptor systems. A plot of χ vs. T^{-1} gives a Curie constant, C, of 1.2×10^{-4} emu K/mol for DDQ° and 4.0×10^{-4} emu K/mol for DMeFc° corresponding to 300 and 1000 ppm $S = {}^1/_2$ impurity or 30 and 100 ppm ($S = {}^5/_2$) iron impurity, respectively.

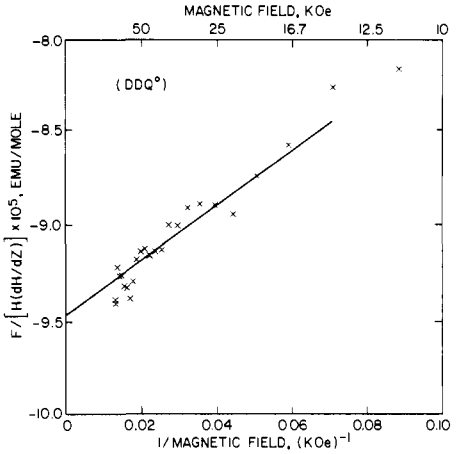

Figure 9. Honda plot for DDQ° (F = force, H = magnetic field, dH/dz = magnetic field gradient).

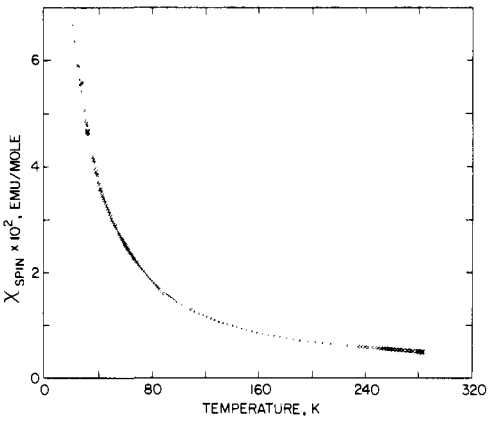

Figure 10. Spin susceptibility vs. temperature for (DMeFc)(DDQH).

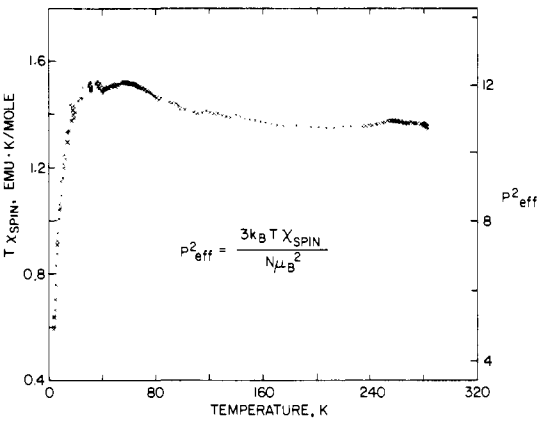

Figure 11. Product of temperature times the spin susceptibility (left-hand scale) vs. temperature for (DMeFc)(DDQH). The square of the effective moment per (DMeFc)(DDQH), p^2, is displayed in the right-hand scale.

As a result of these analyses the core diamagnetism of DDQ° was established as $-0.95 \pm 0.03 \times 10^{-4}$ emu/mol. For DMeFc°, the core diamagnetism was established as -2.30 0.05 $\times 10^{-4}$ emu/mol. Hence, the diamagnetic core for (DMeFc)(DDQ) is -3.25×10^{-4} emu/mol. The presence of an additional hydrogen in (DMeFc)(DDQH) increases diamagnetic core correction[22] by -2×10^{-6} emu/mol to -3.27×10^{-4} emu/mol. The spin susceptibility, χ_{spin}, is readily obtained from the measured susceptibility, χ_{meas}, i.e.,

$$\chi_{spin} = \chi_{meas} - \chi_{core} \quad (4)$$

The variation of χ_{spin} with temperature is shown in Figure 10 for measurements taken at 7.585 T on a polycrystalline sample of (DMeFc)(DDQH). The data in Figure 10 are replotted as the

product of temperature and spin susceptibility vs. temperature in Figure 11.

It is seen that $T\chi_{spin}$ increases by 10% as the temperature is decreased from 282 to 40 K. Below 30 K, $T\chi_{spin}$ decreases monotonically. Assuming a Curie law for independent magnetic moments,

$$T\chi_{spin} = Np^2\mu_B{}^2/3k_B \quad (5)$$

where N is the number of spin sites, μ_B is the Bohr magneton, and k_B is Boltzmann's constant. The effective moment per site, p, is given by

$$p^2 = g^2J(J + 1) \quad (6)$$

where g is the spectroscopic splitting factor and J is the total angular momentum per site. The right-hand scale for Figure 11 is in units of p^2 [$p^2 = 3k_B\chi_{spin}T/(N\mu_B{}^2)$]. The value for p^2 varies from 11.0 at room temperature to 12.2 at 30 K. The experimental value of p^2 may be taken as a sum of the p^2 for the individual sites for independent spins; hence,

$$p^2 = p^2{}_{DMeFc} + p^2{}_{DDQ} \quad (7)$$

It has previously been shown that the g value for ferrocenes as well as $DMeFc^{+\cdot}$ is very anisotropic. Values for $g_\parallel$ are generally $\sim$4, with values as high as 4.40 having been reported in some $DMeFc^{+\cdot}$ compounds.[5,21,23] In contrast $g_\perp$ for $DMeFc^{+\cdot}$ is $\sim$1.92.[5,21,23] If α is defined as the fraction of DMeFc whose major axis is parallel to the magnetic field, then

$$p^2{}_{DMeFc} = \alpha p_\parallel{}^2 + (1 - \alpha)p_\perp{}^2 \quad (8)$$

with

$$p_\parallel{}^2 = g_\parallel{}^2J(J + 1) = 4^2(1/2)(3/2) = 12 \quad (9)$$

$$p_\perp{}^2 = g_\perp{}^2J(J + 1) = (1.92)^2(1/2)(3/2) = 2.76 \quad (10)$$

The experimentally determined $p^2 = 11.0$ at 280 K can be used to assign the location of spins in the (DMeFc)(DDQH) solid.

Two extreme cases are examined. Both models assume independent spins with no interaction (exchange) among the spins.

(a) The spin state of each DDQ is $S = {}^1/_2$, (i.e., $DDQ^{-\cdot}$) and that of each $DMeFc^{+\cdot}$ is $S = {}^1/_2$. In this case $p^2{}_{DDQ} = 3.0$, implying $p^2{}_{DMeFc} = 8.0$. When eq 8–10 are used, consistency requires that $\alpha = 0.57$, that is, that the $DMeFc^{+\cdot}$ are preferentially aligned with the major axis parallel to the magnetic field. This partial alignment of the polycrystalline powder may occur during the upfield scan at 280 K. However, for low magnetic fields (<1 T) the initial apparent experimental susceptibility was approximately one-half the high-field value. With the assumption that the powder sample was initially unoriented, i.e., $\alpha = 0.333$, then with a change to the $\alpha = 0.57$ orientation at 7.58 T, an increase of χ_{spin} by 16%, not 100%, is expected.

(b) An alternate approach is suggested by previous experiences with powder samples with high anisotropy. It has been earlier reported that powder samples of the metamagnetic one-dimensional phase of (DMeFc)(TCNQ) become nearly fully oriented in magnetic field less than 1 T.[5] Since the DDQ product with the DMeFc has a qualitatively similar structure, this case must also be considered. As the observed $p^2 = 11.0$ is close to the $p^2{}_\parallel = 12.0$ for oriented $DMeFc^{+\cdot}$, this model implies that all of the observed spin residues on the DMeFc moiety and that there are no spins on the DDQ. The fraction of crystallites oriented at 7.582 T is, from eq 8, 0.89. The ratio of high-field ($\alpha = 0.89$ oriented) to low-field ($\alpha = 0.33$) susceptibility would then be predicted to be 1.88, in close agreement with experiment.

Examination of Figure 11 reveals that χ_{spin} does not appear quite Curie-like, with a small (11%) increase in p^2 upon cooling from 280 to 75 K. This increase in p^2 may be associated with an effective ferromagnetic exchange interaction, as had been observed for the (DMeFc)(TCNQ) linear chain compound. By fitting the data in this temperature range to a Curie–Weiss law, $\chi_{spin} = C/(T - \theta)$, a good fit was obtained for $\theta = 11.6$ K and $C = 1.27$ emu K/mol ($p^2 = 10.2$). This approach suggests close similarity between (DMeFc)(DDQ) and the metamagnet (DMeFc)-(TCNQ), which has $\theta = 3$ K.

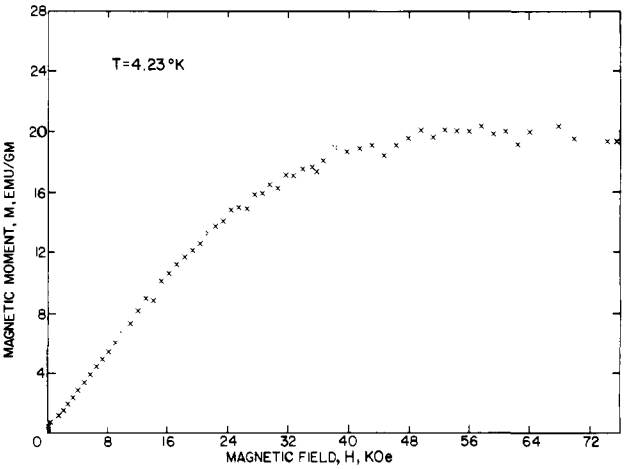

Figure 12. Experimental magnetization as a function of applied magnetic field for (DMeFc)(DDQH) at $T = 4.23$ K.

The second model described above gives an alternative interpretation, however; that is, upon cooling from 280 to 75 K (increasing magnetic moment) the crystals become fully oriented with respect to magnetic field. The observed temperature-independent p^2 (35 K < T < 75 K) of 12.01 is the expected value for fully aligned crystals with $q_\parallel = 4.00$. These two models may be distinguished through detailed analysis of the magnetic field and temperature variation of the sample magnetization, $M(H,T)$, as seen in Figure 12. The susceptibility continues to increase with decreasing temperature (albeit with decreasing p^2) with no indication of three-dimensional ferromagnetic ordering (divergence of susceptibility). The apparent decrease in p^2 for $T < 30$ K may be indicative of antiferromagnetic ordering [as observed for less than 0.2 T in (DMeFc)(TCNQ)]; however, the variation of M with H observed at 4.23 K, Figure 12, is unusual for an antiferromagnet. The large value of $g_\parallel = 4.00$ of $DMeFc^{+\cdot}$ and high magnetic fields used require that $M(H,T)$ be analyzed in terms of the Brillouin function for $T < 30$ K. For $J = {}^1/_2$ systems,

$$M = \sum_i N_i g_i J\mu_B \tanh(x_i) \quad (11)$$

$$x_i = \mu_i H/k_B T = g_i J\mu_B/k_B T \quad (12)$$

and N_i, g_i, and μ_i refer to the number, g factor, and magnetic moment of each type spin site i. For ($DMeFc^{+\cdot}$)($DDQH^-$) there are three terms in the sum in eq 11; i.e., $g = 2$ for $DDQH^-$ and $g_\parallel = 4.00$ and $g_\perp$ and $g_\perp = 1.92$ for DMeFc. These $g_\parallel$ and $g_\perp$ are those reported for $(DMeFc)(PF_6)$.[23]

When $p^2 = 12.01$ obtained for 30 K < T < 70 K is utilized and one spin ${}^1/_2$ per DDQ is assumed, the fraction of DMeFc oriented with the major magnetic axis parallel to H is 0.675 (i.e., 0.325 of the DMeFc is in the perpendicular orientation). Equation 11 can now be evaluated, with the results plotted in Figure 13 (shorted dashed curve) together with the experimental data (x's). There is an excellent agreement with this data below 40 kOe (4.0 T). Above this field the measured magnetic moment, M, is *less* than that predicted (disagreeing by 25% at 7.5 T). If instead α is equal to 0.2 (20% of $DMeFc^{+\cdot}$ aligned parallel to the magnetic field) with an independent spin ${}^1/_2$ on each DDQ, then the magnetic moment predicted by eq 8 agrees with the experimental results at 7.5 T but is too low at low fields (dotted line in Figure 13).

The ambiguity in interpretation of higher temperature data and the unusual $M(H)$ at 4.23 K are now readily resolved. Assuming all (DMeFc)(DDQH) crystallites align parallel to H and that the spin susceptibility of $DDQH^-$ is suppressed, $M(H)$ for $T = 4.23$

(21) Duggan, D. M.; Hendrickson, D. N. *Inorg. Chem.* **1975**, *14*, 995.
(22) Mulay, L. N.; Boudreaux, E. A. "Theory and Applications of Molecular Diamagnetism"; Wiley: New York, 1976.
(23) Goan, J. C.; Berg, E.; Podall, H. E. *J. Org. Chem.* **1964**, *29*, 975.

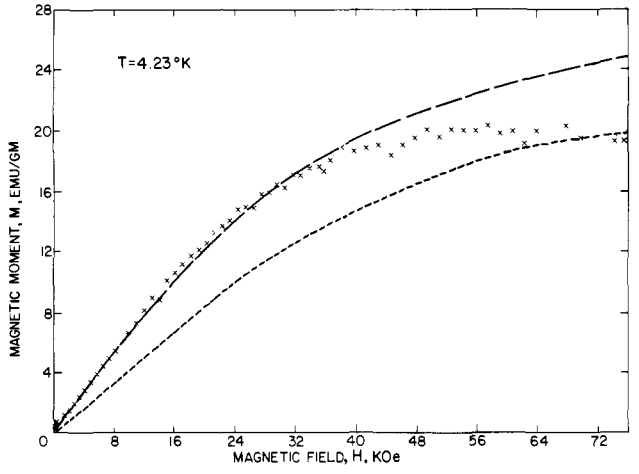

Figure 13. Magnetization vs. field at T = 4.23 K, predicted assuming independent spins on DMeFc and DDQ moieties (see text). The x's are the experimental data. The dashed line is the Brillouin function, assuming spin $^1/_2$ with g = 2 for each DDQ, 0.675 of the DMeFc aligned parallel to the magnetic field with g = 4.0, and 0.325 of the DMeFc aligned perpendicular to the magnetic field with $g_\perp$ = 1.92. The dotted line is the Brillouin function assuming spin $^1/_2$ with g = 2 for each DDQ, 0.20 of the DMeFc aligned parallel to the magnetic field with $g_\parallel$ = 4.0, and 0.80 of the DMeFc aligned perpendicular to the magnetic field with g = 2.0.

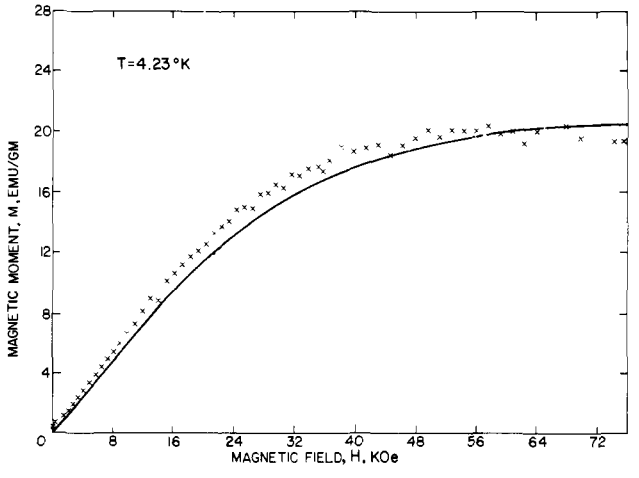

Figure 14. Magnetization vs. field at T = 4.23 K. The ×'s are the experimental data. The solid curve is the Brillouin function, assuming spin $^1/_2$ with $g_\parallel$ = 4.0 on each DMeFc and no spin on the DDQH moiety.

K is simply determined (Figure 14). An excellent qualitative and quantitative fit to the data is obtained for one spin per (DMeFc⁺·)(DDQH⁻) formula unit with $g_\parallel$ = 4.00. The small deviation observed at approximately 2.5 T probably reflects a slightly larger intrinsic g value.

For further verification of this assignment, the low-temperature dependence of χ and M are examined. Experiments were performed for H < 0.7 T (where eq 11 reduces to a simple Curie law for *no* coupling between spins) for temperatures as low as 1.80 K. The measured $\chi(T)$ was found to follow a simple Curie behavior with p^2 constant at 12.1. No sign of ferromagnetic or antiferromagnetic coupling was observed for all H and T examined.

The Brillouin function is sensitive to temperature as well as magnetic field. Figure 15 is a plot of the apparent spin susceptibility (M/H) vs. log T for 4.2–40 K together with the prediction of eq 11, assuming one spin with $g_\parallel$ = 4.00 per (DMeFc)(DDQH) formula unit. The qualitative and quantitative fit is excellent.

Discussion

Since our report[5] of the metamagnetic properties of (DMeFc⁺·)(TCNQ⁻·), we have been looking for alternative metamagnetic systems. It was our hope to prepare a 1:1 salt from

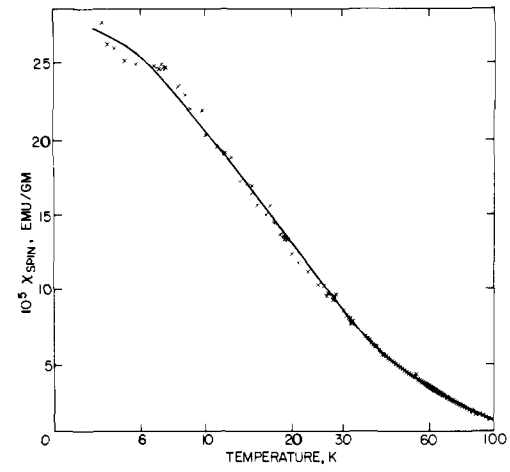

Figure 15. Apparent spin susceptibility (M/H) vs. temperature for H = 7.582 T and 4.2 K < T < 40 K. The solid line is the variation predicted by the Brillouin function, assuming only spins on the DMeFc with $g_\parallel$ = 4.00.

Table V. Comparison of the Interatomic Distances (Å) in DDQ°, DDQ⁻·, and DDQH⁻

atoms	DDQ°[24a]	DDQ°[25a]	DDQ°[25b]	DDQ⁻·[24b]	DDQH⁻
C(6)–C(6')	1.339 (4)	1.350	1.344	1.363 (4)	1.368 (5)
C(6')–C(7')	1.481 (4)	1.499	1.490	1.455 (4)	1.454 (3)
C(7')–C(8')	1.502 (4)	1.502	1.477	1.451 (4)	1.445 (3)
C(8')–C(8)	1.343 (4)	1.334	1.345	1.386 (4)	1.384 (4)
C(8)–C(7)	1.491 (4)	1.499	1.502	1.437 (4)	1.445 (3)
C(7)–C(6)	1.483 (4)	1.484	1.458	1.471 (4)	1.454 (3)
C(7)–O	1.206 (3)	1.222	1.214	1.248 (3)	1.247 (3)
C(7')–O	1.199 (3)	1.208	1.203	1.244 (4)	1.247 (3)
C(6)–Cl	1.698 (3)	1.715	1.732	1.717 (3)	1.732 (2)
C(6')–Cl	1.695 (3)	1.707	1.741	1.714 (3)	1.732 (3)
C(8)–C(9)	1.442 (4)	1.439	1.455	1.435 (4)	1.438 (3)
C(8')–C(9')	1.429 (4)	1.460	1.503	1.425 (5)	1.438 (3)
C(9)–N	1.133 (4)	1.144	0.95	1.135 (4)	1.101 (3)
C(9')–N'	1.135 (4)	1.127	0.95	1.144 (4)	1.101 (3)
O–H					1.04

aprotic media that was isostructural to (DMeFc⁺·)(TCNQ⁻·). We succeeded in the preparation, and high susceptibility is observed; however, the material is not metamagnetic. The intrachain interplanar C_5–DDQH⁻ separation is 3.564 Å. This is 0.11 Å shorter than that observed for (DMeFc)(TCNQ), i.e., 3.67 Å.

The reaction of ferrocene and 2,3-dichloro-5,6-dicyanoquinone has been postulated to result in a charge-transfer complex containing ferrocenium radical cations and a phenoxy radical anions.[9,23] Later the anion was predicted to be DDQH⁻.[12] Evidence for the phenoxy radical was based on the disappearance of the 1680-cm⁻¹ carbonyl stretching vibration, the enhancement of the 2230-cm⁻¹ absorption assigned to $\nu_{C\equiv N}$ of the nitrile group, and the appearance of an absorption at 1590 cm⁻¹ assigned to the phenoxy radical.[9] However, interpretation of magnetic susceptibility data led Hendrickson and co-workers to suggest that the DDQ moiety is diamagnetic and should be postulated as DDQH⁻.[12] From our experimental magnetic data and the appearance of a peak at the correct position for a quinone-like hydrogen in the electron density maps, we believe that the radical anion is not found, but rather the proposed DDQH⁻ anion is present.

A comparison of the bond distances within DDQH⁻ with the recently reported values for DDQ·[24a,25] and DDQ⁻·[24b] is shown in Table V. The bond distances within DDQH⁻ are very similar to those reported for the DDQ⁻· ion[24b] except for the differences in the C—Cl and C≡N bond distances. The C—Cl bond distances appears to have lengthened while the C≡N bond distance

(24) (a) Zanotti, G.; Bardi, R.; Del Pra, A. *Acta Crystallogr., Sect. B* **1980**, *36*, 168. (b) Zanotti, G.; Del Pra, A. *Ibid.* **1982**, *38*, 1225.

(25) (a) Herbstein, F. H.; Kapon, M.; Rjonjew, G.; Rabinovich, D. *Acta Crystallogr., Sect. B* **1978**, *B34*, 476. (b) Bernstein, J.; Regen, H.; Herbstein, F. H. *Ibid.* **1977**, *B33*, 1716.

is shorter than the expected value. A similar result was observed for the benzophenanthrene–DDQ° material[25b] where a positional disorder occurs between two DDQ° orientations such that excess electron density appeared between the carbon and nitrogen atoms of the C≡N bonds due to the Cl atoms of the second orientation. The occupancy of the two orientations was approximately 80:20, leading to a poor C≡N refinement. In our final difference Fourier electron density map, we see electron density at the noise level of the map (0.53 e/Å^3) at a position between the carbon and nitrogen atoms of the C≡N bonds. Therefore, we believe that there exists a minor orientation of the $DDQH^-$ that would disorder the Cl and C≡N substituents, causing slight bond-distance deviations from the normal values. The C—Cl bonds are therefore anomalously long while the C≡N bonds are shortened by this effect.

With the above disorder taken into account, there are no significant differences in bond distances between the $DDQ^{-}\cdot$ ion[24b] and the $DDQH^-$ we are reporting except the observation of electron density in a position to be assigned to that of a hydrogen atom bound to the quinone oxygen. This observation fits the conclusion drawn from the magnetic data for various $DDQH^-$ materials. Since no precautions were taken to alleviate moisture in the preparation of the $DDQ^{-}\cdot$[24b] anion, there is a possibility that the hydrogen atom position was overlooked on the electron density maps and that it is also $DDQH^-$.

There are significant differences between the $DDQH^-$ and DDQ° molecules, which have been reported as Table V displays. The C–C distances of the quinone ring in $DDQH^-$ tend toward that of a benzenoid system but still retain much of the quinone character. A further shift of approximately 0.04–0.05 Å is needed to reach equivalence (1.395 Å). These distances are therefore intermediate between the benzenoid and quinoid states. The quinone C=O bonds have lengthened significantly on electron addition but still have not reached the single C—O bond value of 1.35 Å found in hydroquinone structures.[26]

The six-membered ring has become more planar than in the DDQ neutral structure, where a definite boat configuration has been observed.[24] This result is yet another indication of the resulting intermediate benzenoid/quinone structure. All of these points imply that the added electron is delocalized over much of the molecule.

The decamethylferrocenium ion has been characterized previously[6,8] and shows average Fe–C, C–C, and C–Me bond distances of 2.090 (7), 1.418 (6), 1.502 (6) Å, which can be compared to the average distances observed in $[DMeFc^{+}\cdot][DDQH^-]$ of 2.096 (2), 1.422 (3), and 1.505 (3) Å. These distances are longer than those reported for neutral decamethylferrocene,[27] where the average distances of 2.050 (2), 1.419 (2), and 1.502 (3) Å are observed. The main difference is the Fe–C bond length, which has increased substantially on the removal of a single electron.[30] All C_5 bond distances are essentially equivalent—ranging from 1.48 (3) Å to 1.424 (3) Å. The C_5Me_5 rings are staggered with a twist angle of 26°.

The stacking of alternating $[DMeFc]^{+}\cdot[DDQH]^-$ ions along the *c* axis provides a heterosoric interaction of ions,[28] which in a similar material has been shown to possess unusual magnetic properties in the form of metamagnetism.[5,7,8a] In the 1:1 charge-transfer complex of decamethylferrocene and TCNQ, two phases result at room temperature, one being dimeric and the other showing heterosoric stacked ions along the crystalline *c* axis, giving rise to a stacking distance of 3.67 (2) Å between the $TCNQ^-$ and the C_5Me_5 ring of $DMeFc^{+}\cdot$ ion.[8a] In $(DMeFc^{+}\cdot)(DDQH^-)$, the stacking distance is 3.564 Å between these planes; however, the magnetism as previously discussed is quite different.[5,8a] The packing of ions within the crystalline lattice is similar in both materials whereas there are alternating ions in two of the crystallographic directions and like ion neighbors in the third direction. The separation of the Fe atoms in the stacking direction is 10.616 Å, which is shorter than that reported for the analogous metamagnetic $(DMeFe)^{+}\cdot(TCNQ)^{-}\cdot$ complex of 10.840 (5) Å.[8] This corresponds to the difference in stacking distance of the cation/anion since the Fe–C_5Me_5 distance is essentially the same in both materials.

The 1:1 ferrocene tetracyanoethylene complex also possesses a similar structural array; however, complete charge transfer is not achieved for this diamagnetic substance.[29]

Conclusion

For the $(DMeFc^{+}\cdot)(DDQH^-)$ materal, it is clear from the magnetic studies that the observed spins are only on the $DMeFc^{+}\cdot$ moiety and that they act independently. This is in marked contrast to the metamagnetic $(DMeFc^{+}\cdot)(TCNQ^{-}\cdot)$ material, which has very different temperature dependence of the magnetic properties. This presumably arises from the presence of both radical cation and anions in $(DMeFc^{+}\cdot)(TCNQ^{-}\cdot)$ and only radical cations in $(DMeFc^{+}\cdot)(DDQH^-)$. Thus, the presence of spins on the $TCNQ^{-}\cdot$ must enable the exchange coupling between $DMeFc^{+}\cdot$ moieties leading to metamagnetic behavior. The lack of an intervening radical anion in $(DMeFc^{+}\cdot)(DDQH^-)$ leads to independent behavior for the $DMeFc^{+}\cdot$ spins.

Registry No. $[DMeFe^+][DDQH^-]$, 82135-50-0; DMeFe, 12126-50-0.

Supplementary Material Available: Structure factor table for $C_6(CN)_2Cl_2O_2H\cdot Fe[C_5(CH_3)_5]_2$ (15 pages). Ordering information is given on any current masthead page.

(26) Sakurai, T. *Acta Crystallogr.* **1962**, *15*, 443.
(27) Freyberg, D. P.; Robbins, J. L.; Raymond, K. N.; Smart, J. C. *J. Am. Chem. Soc.* **1978**, *101*, 892.
(28) Dahm, D. J.; Horn, P.; Johnson, G. R.; Miles, M. G.; Wilson, J. D. *J. Cryst. Mol. Struct.* **1975**, *5*, 27.
(29) Adman, E.; Rosenblum, M.; Sullivan, S.; Margulis, T. N. *J. Am. Chem. Soc.* **1967**, *89*, 4540. Rosenblum, M.; Fish, R. W.; Bennett, C. *Ibid.* **1964**, *86*, 5766.
(30) Haaland, A. *Top. Curr. Chem.* **1975**, *53*, 1.